Journal of Magnetic Resonance 198 (2009) 252–260

Contents lists available at ScienceDirect

Journal of Magnetic Resonance

journal homepage: www.elsevier.com/locate/jmr

Spin echo SPI methods for quantitative analysis of fluids in porous media

Linqing Li [a,b], Hui Han [a], Bruce J. Balcom [a,b,*]

[a] MRI Centre, Department of Physics, P.O. Box 4400, University of New Brunswick, Fredericton, NB, Canada E3B 5A3
[b] Department of Chemistry, P.O. Box 4400, University of New Brunswick, Fredericton, NB, Canada E3B 5A3

ARTICLE INFO

Article history:
Received 4 September 2008
Revised 2 March 2009
Available online 9 March 2009

Keywords:
MRI
Spin echo single point imaging
SE-SPI
Density imaging
Core analysis
T_2 distribution
Irreducible water saturation
NMR well logging
Coates equation

ABSTRACT

Fluid density imaging is highly desirable in a wide variety of porous media measurements. The SPRITE class of MRI methods has proven to be robust and general in their ability to generate density images in porous media, however the short encoding times required, with correspondingly high magnetic field gradient strengths and filter widths, and low flip angle RF pulses, yield sub-optimal S/N images, especially at low static field strength. This paper explores two implementations of pure phase encode spin echo 1D imaging, with application to a proposed new petroleum reservoir core analysis measurement.

In the first implementation of the pulse sequence, we modify the spin echo single point imaging (SE-SPI) technique to acquire the k-space origin data point, with a near zero evolution time, from the free induction decay (FID) following a 90° excitation pulse. Subsequent k-space data points are acquired by separately phase encoding individual echoes in a multi-echo acquisition. T_2 attenuation of the echo train yields an image convolution which causes blurring. The T_2 blur effect is moderate for porous media with T_2 lifetime distributions longer than 5 ms. As a robust, high S/N, and fast 1D imaging method, this method will be highly complementary to SPRITE techniques for the quantitative analysis of fluid content in porous media.

In the second implementation of the SE-SPI pulse sequence, modification of the basic measurement permits fast determination of spatially resolved T_2 distributions in porous media through separately phase encoding each echo in a multi-echo CPMG pulse train. An individual T_2 weighted image may be acquired from each echo. The echo time (TE) of each T_2 weighted image may be reduced to 500 μs or less. These profiles can be fit to extract a T_2 distribution from each pixel employing a variety of standard inverse Laplace transform methods. Fluid content 1D images are produced as an essential by product of determining the spatially resolved T_2 distribution. These 1D images do not suffer from a T_2 related blurring.

The above SE-SPI measurements are combined to generate 1D images of the local saturation and T_2 distribution as a function of saturation, upon centrifugation of petroleum reservoir core samples. The logarithm mean T_2 is observed to shift linearly with water saturation. This new reservoir core analysis measurement may provide a valuable calibration of the Coates equation for irreducible water saturation, which has been widely implemented in NMR well logging measurements.

1. Introduction

Quantitative MRI methods applied to porous media have the potential to determine a wide variety of valuable petro-physical properties [1]. Most MRI methods feature inherent relaxation time contrast and in many instances this is considered a positive feature. However, core analysis of fluid properties of porous media frequently requires true fluid content images [2].

The SPRITE class of MRI methods have proven to be robust and general in their ability to generate fluid content images [3] in porous media. However the short encoding times required, with correspondingly high magnetic field gradient strengths and filter widths, and low flip angle RF pulses, yield sub-optimal S/N images, especially at low static field strength.

Spin echo single point imaging (SE-SPI) has inherently good S/N due to a relatively narrow signal bandwidth [4]. Lacking magnetic field gradients at the k-space origin, the imaging experiment will not suffer significant diffusive attenuation [5]. In previous work, SE-SPI has proven very successful in cases where the inherent S/N is poor, such as natural abundance ^{13}C imaging [6], ^{13}C gas phase imaging [7] and high resolution thin film imaging [8]. In addition, as a pure phase encoding technique, SE-SPI will be largely immune to image distortion due to susceptibility variation and paramagnetic impurities in porous media.

A simple density image of fluid distribution in porous media, with no relaxation time contrast, is remarkably difficult to achieve with conventional methods. Short transverse relaxation lifetimes

* Corresponding author. Address: MRI Centre, Department of Physics, P.O. Box 4400, University of New Brunswick, Fredericton, NB, Canada E3B 5A3. Fax: +1 (506) 453 4581.
E-mail address: bjb@unb.ca (B.J. Balcom).

1090-7807/$ - see front matter © 2009 Elsevier Inc. All rights reserved.
doi:10.1016/j.jmr.2009.03.002

(T_2) yield signal loss while multi exponential T_1 and T_2 yield variable signal attenuation in a simple spin echo image. One goal of this work is the achievement of true fluid content images through observing the signal intensity at near zero evolution time.

In the present work the SE-SPI and turbo SE-SPI methods [9] are modified to create a new imaging technique, termed hybrid SE-SPI. The k-space origin data point is acquired with a near zero evolution time from the FID following the 90° excitation pulse. At $k = 0$, no gradient is applied and the $k = 0$ data point has a pure density weighting. Subsequent k-space data points do suffer from T_2 attenuation but the echo time may be reduced to 500 μs or less with rapid gradient switching. T_2 attenuation of the pure phase encoded echoes introduces a convolution to the subsequent density weighted image. In hybrid SE-SPI T_2 is no longer an uncontrolled contrast parameter, it is a blurring parameter.

While fluid content is important for quantitative analysis of porous media, the most common MR measurement in porous media is a relaxation time distribution measurement [10]. Such measurements can determine the pore size distribution over several orders of magnitude in [11]. Properties derived from the NMR-determined pore size distribution include hydraulic permeability, capillary bound water saturation, residual oil saturation and gas volume [12]. Permeability prediction from the T_2 distribution has been adopted as a successful reservoir well logging technology [13].

This work also proposes a new implementation of SE-SPI, termed T_2 mapping SE-SPI, which permits fast 1D T_2 weighted images for the determination of spatially resolved T_2 distributions in porous media. It also features echo times which may be reduced to 500 μs or less. T_2 weighted profiles may then be fit to extract a T_2 distribution, pixel by pixel, employing a variety of standard inverse Laplace transform methods. Fluid content 1D images are produced as an essential by product of determining the spatially resolved T_2 distribution. These 1D images do not suffer from a T_2 related blurring.

The value of a spatially resolved T_2 measurement in reservoir core analysis is demonstrated through measurement of a centrifuged reservoir core plug. A linear relationship between the local water saturation and the logarithm mean T_2 is observed. The linear relationship is predicted based on a simple derivation. The linear relationship produces a fast calibration procedure for the Coates equation describing the irreducible water saturation (SWIRR) of importance to NMR well logging. Compared to the traditional SWIRR calibration procedure [14], the new method should be significantly faster, simpler, more reliable and accurate.

2. Theory

2.1. Hybrid spin echo SPI

The hybrid SE-SPI pulse sequence, Fig. 1a, is capable of obtaining near zero relaxation time weighted images of fluids in porous media. The 1D k-space points are acquired in two separate acquisitions with a 5 times T_1 delay between them to ensure full longitudinal magnetization recovery, and no T_1 weighting.

The phase encoding for each echo is removed by an identical gradient pulse of altered sign immediately after the echo. Each k-space acquisition starts from $k = 0$ then proceeds to higher order k-space points in the positive or negative direction. The two k-space segments may then be combined into a 1D k-space data set for Fourier transformation and image reconstruction. The $k = 0$ data point is the averaged value from the two acquisitions. The overall image intensity is determined by the intensity of the $k = 0$ data point. Frequency encoded or phase encoded spin echo images have a local image intensity defined by Eq. (1).

$$S(y) = \rho_0(y) \exp\left(-\frac{nTE}{T_2(y)}\right) \tag{1}$$

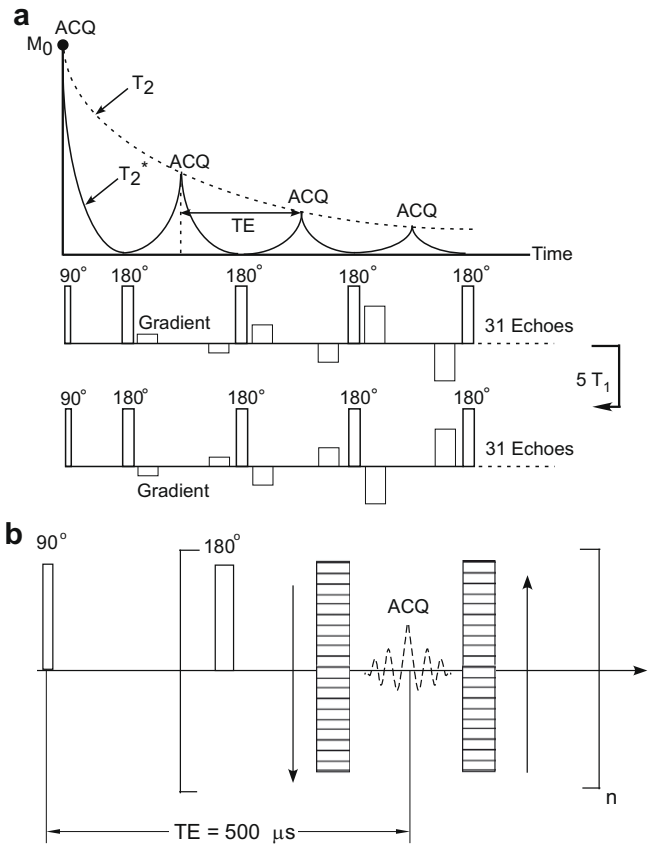

Fig. 1. (a) 1D hybrid SE-SPI pulse sequence for fluid content imaging of fluids in porous media. The $k = 0$ point is taken at a very short evolution time on the FID. Subsequent k-space points are taken from individual pure phase encoded echoes with the phase unwrapped following each echo. (b) 1D spatially resolved T_2 mapping measurement. The echo time in each case was 500 μs. The phase encoding and phase unwinding gradients are applied around each echo with simple CPMG refocusing.

In Eq. (1), n is the echo number corresponding to the center of k-space, while TE is the echo time. The image intensity $S(y)$ is defined by the product of the spin density, $\rho_0(y)$, and T_2 weighting in the exponential term. From Fig. 1a, the T_2 weighting will be simply removed due to taking the first point of the free induction decay (FID) as $k = 0$. In this case, n is equal to zero such that the intensity $S(y)$ in Eq. (1) will be simply equal to the spin density $\rho_0(y)$.

2.2. Blurring in hybrid SE-SPI

Amplitude modulation of the true k-space data, defined by the modulation transfer function (MTF), leads to blurring and other image artifacts. The pulse sequence of Fig. 1a will lead to an exponential decay of the modulation transfer function, and a simple image blurring. The blurring may be quantified by the point spread function (PSF). Severe blurring may cause sufficient degradation that it will affect quantification of hybrid SE-SPI images. The overall MTF and PSF are determined by Eqs. (2) and (3) where the multiplications in Eq. (2) become convolutions in Eq. (3).

$$MTF = MTF_{k\text{-space}} \times MTF_{\text{diffusion}} \times MTF_{T_2} \tag{2}$$

$$PSF = PSF_{k\text{-space}} \otimes PSF_{\text{diffusion}} \otimes PSF_{T_2} \tag{3}$$

$\text{MTF}_{k\text{-space}}$ is the MTF due to k-space sampling, usually with 64 data points. MTF_{T_2} is due to the signal amplitude decay with time constant T_2. Because acquisition of the MTF_{T_2} function is symmetric,

the corresponding PSF will be Lorentzian (for single exponential T_2). $MTF_{diffusion}$ is the MTF due to molecular diffusion through underlying magnetic field gradients which will be limited by decreasing the echo time (TE). Ideally, the limiting resolution will be simply determined by the size of the sampled *k*-space. The most significant blurring in hybrid SE-SPI image will be due to the MTF_{T_2}, and PSF_{T_2} depending on the weighting of the short T_2 components in the T_2 distribution. Decreasing the experimental echo time will attenuate the decay and decrease the blurring.

2.3. T_2 mapping spin echo SPI

To generate spatially resolved T_2 distributions, one must have the ability to generate hundreds or thousands of profiles with very short echo times. The key problems in multi-echo MRI are well known [15]. Deviation from exact 180° refocusing pulses results in image artifacts from stimulated echoes. The modulation and cumulative loss of image intensity in successive echoes, and contamination of the T_2 relaxation with a T_1 contribution, must all be considered [16]. With very short echo times, for example 500 μs, eddy current problems due to fast gradient switching will cause significant trouble for high quality images. Consequently, multi-echo imaging is usually restricted to the acquisition of a limited number of echoes with relatively long echo times, and the measured T_2 values may show considerable scatter [17].

Imaging artifacts in multi-echo imaging are often suppressed by the use of spoiling gradients around the 180° pulses [18]. Alternatively, specific RF excitation phase cycles such as MLEV-4, -8 or -16, or XY -4, -8 or -16 [19] can be applied to counteract the cumulative effects of phase errors. The use of spoiling gradients causes cumulative loss of magnetization from successive echoes and after a large number of echoes, the observed T_2 is reduced [20]. These techniques are not employed in the current experiments.

This work also proposes a modified SE-SPI imaging pulse sequence, Fig. 1b for T_2 mapping. The phase encoding and phase unwinding gradients are applied around each echo with simple CPMG refocusing. By applying the phase encoding gradient for each echo, the stimulated echoes due to imperfect 180° pulses will be removed and this will help ensure an accurate T_2 measurement [19].

2.4. T_2 distribution in porous media at low field

Bulk CPMG measurements to determine the T_2 distribution in porous media are usually undertaken with echo times less than 1 ms. Pore size can be determined only when the pore space is saturated with the wetting phase fluid and the relaxation behavior is dominated by surface relaxation [21]. Decreasing the deleterious effects due to diffusion through internal field gradients requires low field measurement with short echo spacing. For rocks, it has been reported that even at low fields, a 1 ms echo time in porous media may change the CPMG decay due to diffusion through internal field gradients [22]. If fluid saturation is reduced, T_1 and T_2 lifetimes are typically shifted to shorter times [23].

3. Results and discussion

3.1. Hybrid SE-SPI

3.1.1. Core plug image by hybrid SE-SPI

A Berea sandstone (sandstone #1) which has a typical sandstone T_2 distribution, Fig 2a, was imaged employing the pulse se-

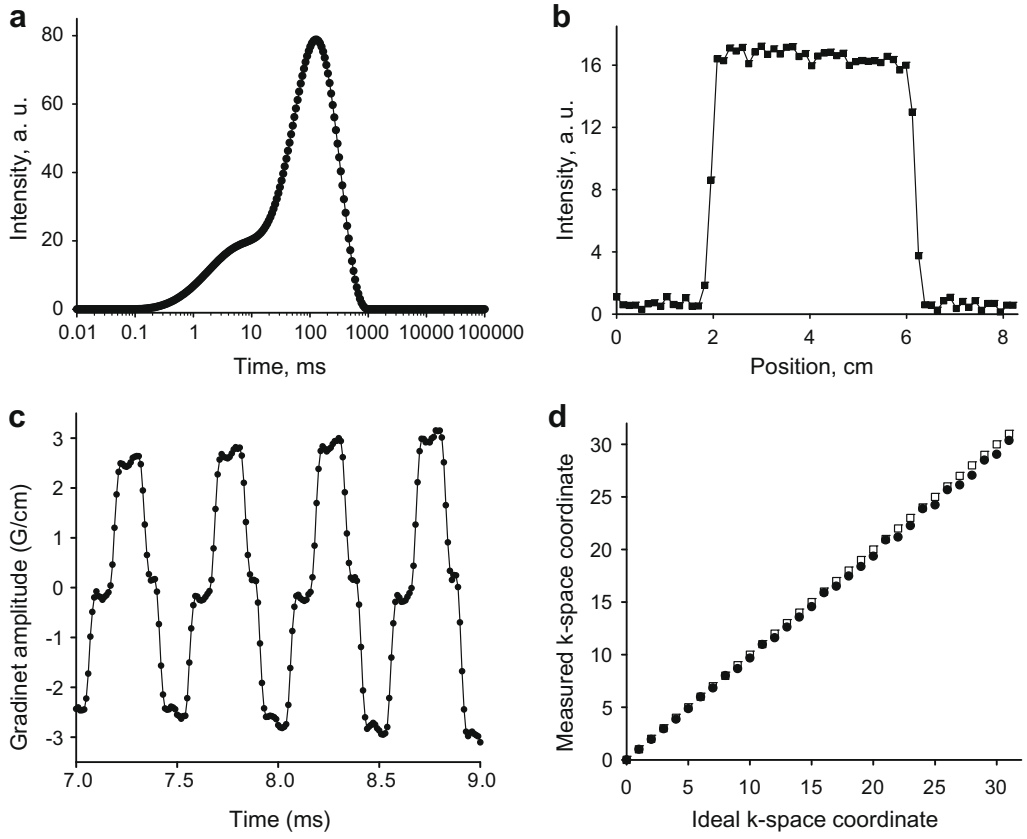

Fig. 2. (a) Bulk T_2 distribution of fully saturated sandstone sample # 1, TE = 500 μs, 1024 echoes. (b) 1D image of sandstone # 1 employing the hybrid SE-SPI technique with TE = 500 μs. (c) Gradient waveform measurement from the 15th to 18th gradient lobes in a hybrid SE-SPI measurement. The gradient waveform is non-ideal but *k*-space sampling is still regular. (d) Integration of the positive gradient *k*-space points, ● matches with the ideal case □.

quence of Fig. 1a. Acquired with 4 scans in 20 s at 0.35 T, the core plug image, Fig. 2b, is a high quality 1D fluid content image with an SNR of 32. As with all experimental and simulated images in this paper, the imaging axis is longitudinal to the sample.

The high quality profile, at short echo time results from the pure phase encoding nature of this experiment. In a phase encoding experiment, it is the increment in gradient area that is most important, not a high fidelity gradient waveform. The gradient waveform was measured employing the methodology of Ref. [24]. Fig. 2c shows that with a phase encoding time (t_p) as short as 150 μs, distortion in the gradient waveform is inevitable. The gradient waveform in Fig. 2c would induce artifacts in a frequency encoding imaging measurement which relies on a constant gradient while sampling k-space.

Unlike frequency encoding techniques, SE-SPI is robust to distortion of the gradient waveform because SE-SPI requires only that the gradient area increment regularly. An integration of the gradient waveform for each positive k-space step is displayed in Fig. 2d and compared to the ideal case. The gradient area increment is close to ideal, as is the gradient cancellation of each phase encode step.

3.1.2. Image sensitivity

The double half k-space 1D SPRITE imaging method (DHK SPRITE) has proven to be a robust and general method to generate fluid content images (spin density images) in porous media [25]. However broad filter widths, and low flip angle RF pulses, yield sub-optimal S/N images. DHK 1D SPRITE and hybrid SE-SPI were employed to image core plug sandstone # 1. We choose, as the basis of comparison, acquisition of images by the two methods signal averaged to equivalent S/N. The sensitivity is defined as

$$\eta = \frac{S/N}{\sqrt{t}} \tag{4}$$

where t is the total imaging time. A sensitivity comparison of the two profiles is shown in Table 1. The sensitivity η differs by a factor of 3. A DHK SPRITE image requires 10 times longer to acquire than a similar hybrid SE-SPI image of these samples at 15 MHz (0.35 T).

The SPRITE filter width in Table 1 is optimal based on the signal bandwidth at k-space extremities. The SE-SPI filter width in Table 1 is however not optimized. It could be narrowed in principle to the natural line width to increase the S/N as $1/\sqrt{FW}$. A potential problem associated with the narrow filter width is, however, an increased receiver deadtime. This dead time could introduce a T_2^* weighting into the images through the FID based $k = 0$ data point. In the current experiment the filter width of 125,000 Hz had a deadtime of 26 μs. This causes minimal T_2^* attenuation of the $k = 0$ data point and is much less than the τ time (250 μs). In general the filter width is more of a T_2^* concern than a limitation on the echo time. It should be possible to design a digital filter for this application which will simultaneously have a narrow bandwidth and short deadtime.

The choice of a SE-SPI filter that is too broad means the sensitivity comparison is even more in favor of SE-SPI than suggested by Table 1. A broad filter width however permits a very simple multiple point echo acquisition for S/N enhancement. A multiple point acquisition on each echo, averaging the resulting data points, is a better strategy for S/N enhancement. To ensure that the noise between data points is uncorrelated, the dwell time between points must be longer than the inverse of twice the filter width [26]. As an example of the potential benefits, the hybrid SE-SPI imaging experiment for sandstone # 1 has a filter width of 125,000 Hz, and therefore a 4 μs dwell time. Based on the gradient waveform measurement of Fig. 2c, the stable gradient period is approximately 50 μs. Therefore at least 10 time domain points on the echo could potentially be acquired for S/N enhancement. This strategy is not implemented in the current work, but will be essential when translating these ideas to low field, 2 MHz, magnets which are industry standard for petroleum reservoir core analysis.

3.1.3. Hybrid SE-SPI T_2 image blurring

T_2 attenuation of the pure phase encoded echoes, illustrated in Fig 1a, introduces a convolution to the subsequent fluid content weighted 1D image. To simulate the extent of the T_2-blurring, a box car function with 5% noise, representing an 1D idealized image, has been calculated in Fig. 3a, 3b. The two boxcar images were convolved with T_2 decays of time constant 2 ms and 5 ms respectively.

The image comparison reveals that the simulated boxcar phantom, convolved with a 2 ms T_2 decay, has an image blurring unacceptable for image quantification. Note the spatial data points on the profile edge are significantly dislocated. The simulated images suggest that hybrid SE-SPI may be employed for porous media with significant T_2 components longer than 5 ms. Typical relaxation times for capillary bound water in petroleum samples are between 3 and 30 ms depending on the rock type [23]. The T_2 relaxation time distribution of Fig. 2a is very common for porous media so we hypothesize that hybrid SE-SPI will be a general tool, although not universal, for fluid content imaging in porous media. Short T_2 components of sandstone sample #1, Fig. 2a, are blurred in the experimental image of Fig. 2b, however, the short relaxation time components are minor and the experimental image is not visibly affected.

Fig. 2b illustrates a successful hybrid SE-SPI 1D image of fluid content in a porous media sample with a relatively long mean T_2. In cases where the mean T_2 is short, hybrid SE-SPI will suffer a serious image blurring. Sandstone # 2 has a relatively short mean T_2 with the T_2 distribution reported in Fig 3c. The experimental hybrid SE-SPI image, Fig. 3d, as expected, shows an unacceptable blur effect.

In samples where short T_2 relaxation time components are important, a centric scan SPRITE experiment is advantageous, or the T_2 mapping SE-SPI experiment outlined below.

3.2. T_2 mapping SE-SPI

By employing the pulse sequence of Fig. 1b, imaging of both sandstone reservoir core plugs was undertaken. The T_2 weighted 1D images of sandstone # 1 are shown in Fig. 4a. 1024 echoes were generated for the T_2 1D weighted images with a 10 min acquisition time. The T_2 weighted 1D images do not suffer the T_2 related blurring of hybrid SE-SPI. The signal intensity decay extracted from a common pixel in each image is displayed in Fig. 4b. Inverse Laplace transformation of this T_2 decay yields the distribution reproduced as Fig. 4c. The bulk T_2 distribution in Fig. 2a and the local T_2 distri-

Table 1
Comparison of hybrid SE-SPI and SPRITE fluid content images for sandstone sample # 1.

Image type	Pulse flip angle	Filter width (Hz)	Acquisition point	Number of scans	S/N	Acquisition time (s)	η[a]
Hybrid SE-SPI	90°	125,000	1	4	32	12	7.15
DHK SPRITE	20°	200,000	1	64	30	137	2.56

[a] η is the sensitivity defined as $\eta = \frac{S/N}{\sqrt{t}}$.

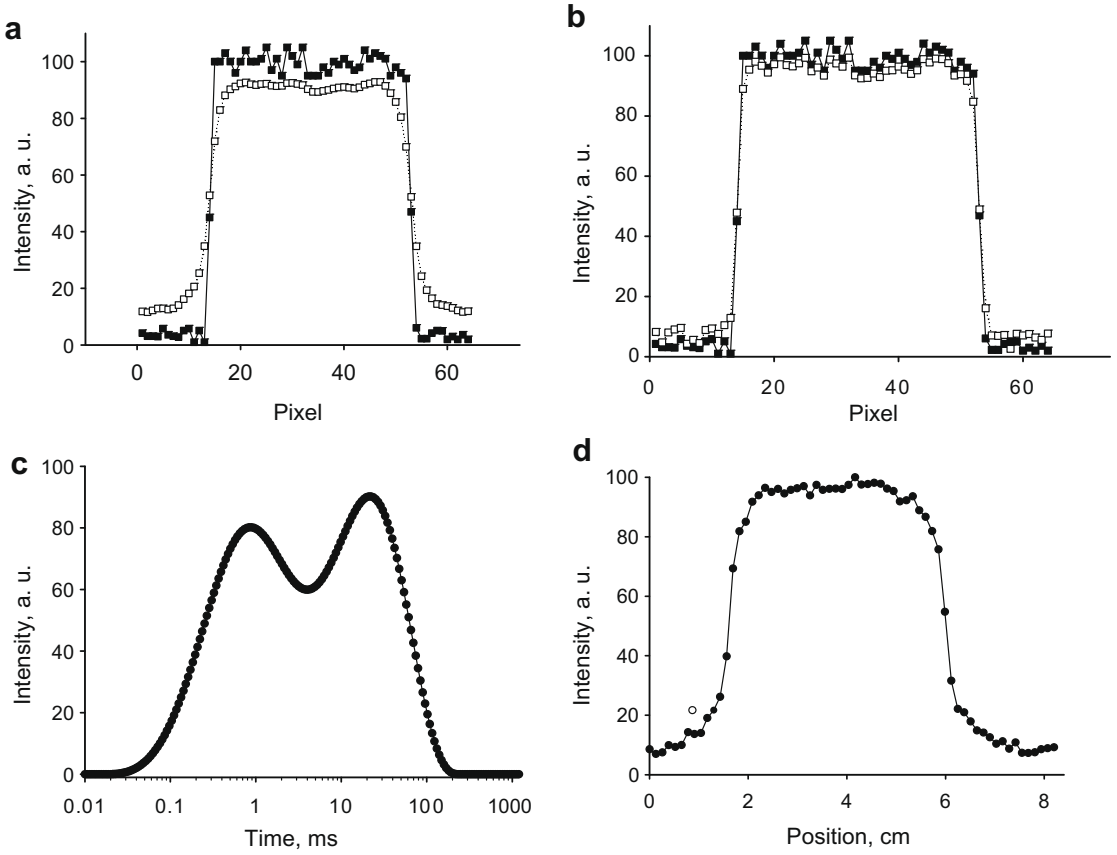

Fig. 3. Simulated 1D images of a simple box car phantom with 5% noise ■. Images □ are the box car phantoms convolved with single exponential T_2 decay, (a) 2 ms T_2 and (b) 5 ms T_2 for measurement with TE = 500 μs. (c) Bulk T_2 distribution of fully saturated sandstone # 2, TE = 500 μs, 256 echoes. (d) Image of sandstone # 2 employing the hybrid SE-SPI technique with TE = 500 μs. Image degradation is similar to that of (a).

bution are nearly identical proving the validity of the T_2 mapping method. Note that an echo time of 500 μs, as employed in this measurement, is similar to the echo times employed in many down-hole NMR logging tools. The T_2 weighted images of sandstone # 2 with shorter T_2, are reproduced in Fig. 4d. Compared to Fig. 3d, a hybrid SE-SPI image, the 1D images of Fig. 4d from T_2 mapping SE-SPI do not suffer from a T_2 related blurring in spite of very short mean T_2. The spatially resolved T_2 distribution, (not shown), is very similar to the bulk T_2 distribution in Fig. 3c.

The pulse sequence of Fig. 1b is an alternate method of generating fluid content images, without edge blurring, but with a much longer image acquisition time than hybrid SE-SPI. A plot of the area under the T_2 distributions for each pixel is a map of fluid content. This provides a simple method of determining fluid content distribution for short T_2 samples when hybrid SE-SPI fails.

3.3. Application of spatially resolved T_2 distribution measurement

The core plug sandstone sample # 1, with T_2 distribution and T_2 weighted profiles shown in Fig. 2a and Fig. 2b respectively, was centrifuged at 500 rpm for 2 h. It was imaged with the method of Fig. 1b to generate T_2 weighted images. Fig. 5a illustrates the centrifugation process. During centrifugation in air, water drains from the left side to right side of the sample. Centrifugation is a common procedure in reservoir core analysis and introduces a spatially varying saturation [27]. The fluid content is higher on the right side of the profile because fluid accumulates at the outlet end of the sample due to capillary pressure effects and the outlet boundary condition. One anticipates from the centrifugation that larger pore sizes will be preferentially emptied due to capillary pressure effects, and that a change in the T_2 distribution should result from this desaturation.

The T_2 signal decay from pixels 20, 30 and 42, marked in Fig. 5b, is displayed in Fig. 5c. Since the experiment was implemented at low field with TE = 500 μs, the diffusion contribution to transverse magnetization decay can be reasonably ignored. The T_2 distribution is thus dominated by the S/V of fluid occupied pores. Fig. 5c clearly reveals that the T_2 relaxation decay shifts to shorter lifetimes as water is removed by centrifugation. In Fig. 5d, an Inverse Laplace Transform was implemented to show the T_2 distribution from chosen pixels along the profiles of Fig. 5b. A shift of the T_2 distribution toward shorter lifetimes with reduced saturation is clearly observed in Fig. 5d. As anticipated, the area under the curve decreases with desaturation. The water does not significantly redistribute in this sample during the measurement duration of 10 min.

3.4. Correlation between the local logarithm mean T_2 and the local saturation

The residual water saturation from each pixel of the core plug can be calculated from the ratio of the exponential fitting result of Fig. 5b and the corresponding pixel amplitude of Fig. 2b (fully saturated image). One could use Fig. 4a to determine the signal amplitude of the fully saturated image, however, the hybrid SE-SPI technique for pure density imaging acquisition is almost 30 times faster than the spatially resolved T_2 measurement.

A linear relationship between the logarithm mean T_2 and the residual water saturation, pixel by pixel, was observed, and is

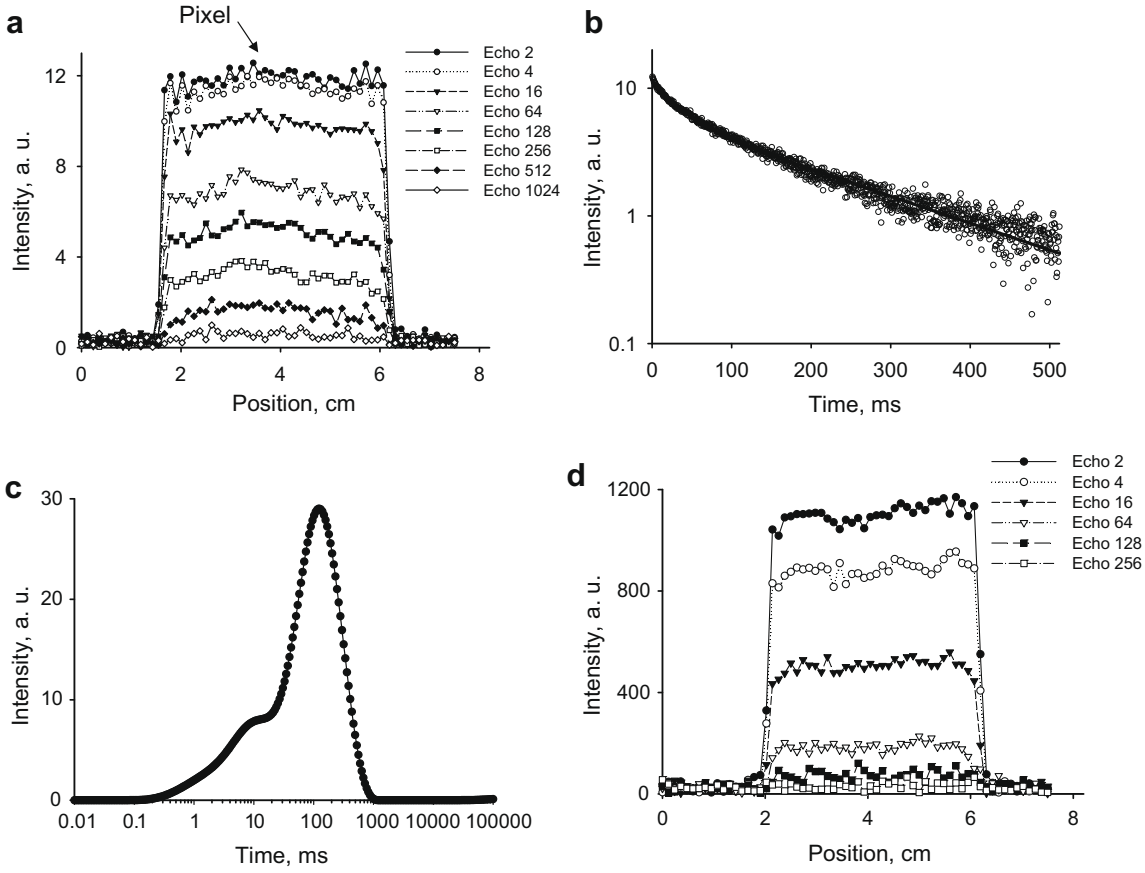

Fig. 4. (a) T_2 weighted images of sandstone # 1 acquired by the T_2 mapping pulse sequence, Fig. 1b, in 10 min with TE = 500 μs. (b) Image intensity decay extracted from the marked pixel in (a), for each T_2 weighted image. A total of 1024 images were collected from 1024 echoes. (c) Inverse Laplace transformation of the T_2 decay data in (b) yields the T_2 distribution. This spatially resolved T_2 distribution is essentially identical to the bulk T_2 distribution, shown in Fig. 2a, in this largely homogenous sample. (d) T_2 weighted images of sandstone # 2 acquired by the T_2 mapping pulse sequence, Fig. 1b, in 5 min with TE = 500 μs, 256 echoes. There is no T_2-blurring effect in these images. The T_2 distribution, spatially resolved, is not displayed but is very close to that of Fig. 3c, the bulk result.

reproduced in Fig. 6a. The logarithm mean T_2, a common NMR core analysis and NMR logging parameter, is defined by Eq. (5).

$$T_{2LM} = \exp\left[\frac{\sum_i [P_i \ln(T_{2i})]}{\sum_i P_i}\right] \tag{5}$$

The probabilities, P_i, are logarithmically spaced amplitudes in the T_2 distribution.

The explanation of this linear relationship is quite straightforward and although outlined only in brief, may provide an important new core analysis measurement.

3.4.1. Empirical model for irreducible water saturation

The irreducible water volume from magnetic resonance logging tools provide the log analyst important information on a formation's permeability and its water-cut potential [14]. Coates et al [14] has derived an equation for the irreducible water saturation (SWIRR) to aid NMR well logging data interpretation. The equation is reproduced as Eq. (6).

$$\frac{1}{\text{SWIRR}} = mT_{2LM} + b \tag{6}$$

SWIRR is the irreducible water saturation (water that can not readily be removed from the sample) while T_{2LM} is the logarithm mean T_2 (ms). The slope and intercept, m and b, are parameters to be determined by a calibration procedure before interpretation of the NMR well logging data.

Following Coates, we derive Eq. (7)

$$\frac{S_{w(T_{2LM})}}{\text{SWIRR}} = mT_{2LM} + b \tag{7}$$

The difference between Coates Eqs. (6) and (7) comes from an alternate definition of the free fluid index (FFI which is free fluid volume). Coates defined FFI as being equal to ϕ(1-SWIRR) by assuming the reservoir rock is fully saturated with porosity ϕ. We define FFI as being equal to $\phi(Sw_{(T_{2LM})}$-SWIRR) since the reservoir rock is partially saturated it contains less free fluid. The $S_{w(T_{2LM})}$ is the local residual water saturation and changes in this value will have associated changes in the logarithm mean T_{2LM} in a rock centrifugation experiment.

According to Coates, in most cases the intercept b in Eq. (6) can be constrained to 1. The same assumption modifies Eq. (7) to Eq. (8).

$$S_{w(T_{2LM})} = m \times \text{SWIRR} \times T_{2LM} + \text{SWIRR} \tag{8}$$

Eq. (8) suggests that a linear relationship between residual water saturation and the T_{2LM} will exist with an intercept that is SWIRR. The m value is determined from the slope of the plot.

3.4.2. MRI fast calibration result for sandstone

Based on Eq. (8), the intercept of Fig. 6a is 22.5 which indicates the SWIRR is 22.5%. The slope of 1.25 leads to an m value of 0.056 ms^{-1}. This experimental m agrees well with Coates' m value of 0.055 ms^{-1} [14] when b was constrained to 1 for sandstones. In

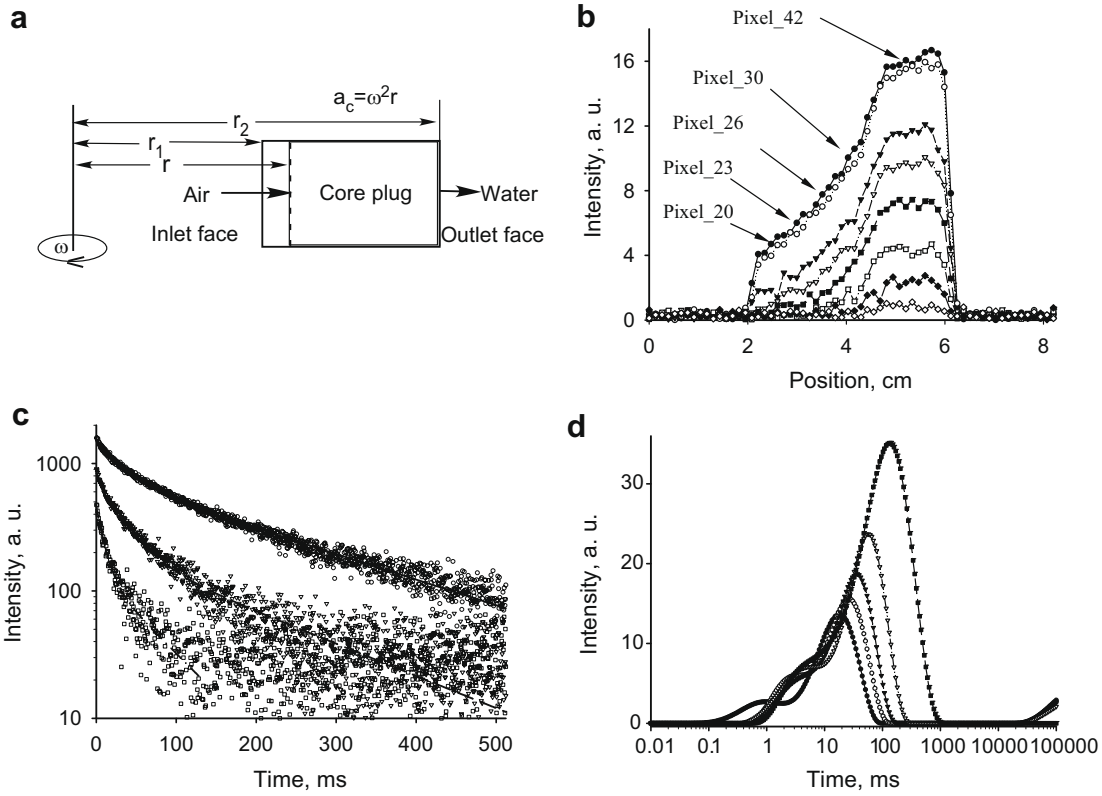

Fig. 5. (a) Schematic of a rock core plug centrifuge experiment. (b) T_2 weighted images of sandstone # 1 acquired after centrifugation with TE = 500 μs, 1024 echoes. Images are displayed for echo numbers ● 2, ○ 4, ▼ 16, Δ 64, ■ 128, □ 256, ♦ 512 and ◇ 1024. (c) Signal decay from pixels □ 20, Δ 30 and ○ 42 extracted from the experiment of (b). (d) Inverse Laplace transform of T_2 decay from pixels 20, 23, 26, 30 and 42 yields T_2 distributions which decrease in amplitude and shift progressively to shorter lifetimes.

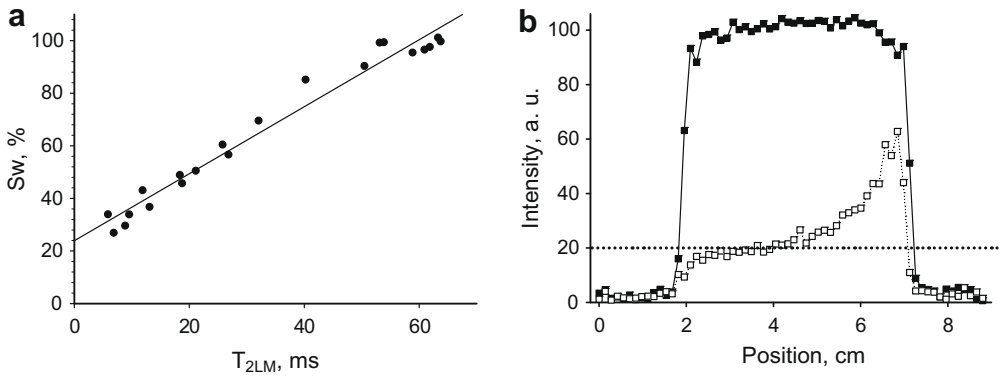

Fig. 6. (a) Local saturation determined from the ratio of the fully saturated hybrid SE-SPI image intensity to the local image intensity. The logarithm mean T_2 is observed to shift linearly with local saturation. The intercept indicates the irreducible water saturation is 22.5%. (b) Hybrid SE-SPI images of fully saturated and desaturated sandstone # 1 (48 h centrifugation at 1000 rpm). The dashed line indicates an SWIRR of 20% which agrees closely with the result of (a).

Coates' work [14], m was determined by bulk NMR measurement of nine different core plugs chosen from medium- to high-porosity sandstone formations. In the same work, Coates determined an m value of 0.0618 ms^{-1} for a larger data set of 340 sandstones.

An alternative way to confirm Eq. (8) is to independently determine the irreducible water saturation of the sandstone employed. Sandstone # 1 was further centrifuged for 48 h at 1000 rpm until an equilibrium state was reached. Hybrid SE-SPI was employed for fluid content imaging of the desaturated rock profile. Once again, fluid accumulates on the right hand side of the profile due to capillary pressure effects and the outlet boundary condition. The fully saturated and desaturated profiles in Fig. 6b indicate that the irreducible water saturation (SWIRR) is approximately 20%. The SWIRR predicted from our MRI calibration procedure agrees reasonably well with the independent measurement of SWIRR.

If *b* is not constrained, then Eq. (7) could be used for the calibration. In this case, the irreducible water saturation SWIRR must be determined before the MRI centrifugation measurement. Once SWIRR is determined, simple linear regression, Eq. (7), will determine the slope (m parameter) and intercept (*b* parameter).

The Coates Eq. (6) for irreducible saturation is a special case of Eq. (7) proposed in this paper. If $S_{w(T_{2LM})}$ in Eq. (7) is equal to 100%, then Eq. (7) will be identical to Eq. (6) proposed by Coates. Both equations can be employed for rocks with a narrow T_2 distribution [14]. For rocks with a broad T_2 distribution, the linear relationship between S_W and logarithm mean T_2 may not be true [28]. The gen-

erality of the new method proposed will be the subject of further investigation.

4. Conclusion

The essential problem in quantitative fluid content MRI of porous media is the ill controlled contrast which results from the T_2 distribution. We proposed a quantitative imaging technique which avoids T_2 contrast, hybrid SE-SPI, and a second method, T_2 mapping SE-SPI, which permits determination of the T_2 distribution spatially resolved.

A short evolution time FID yields the *k*-space origin data point, and the resulting image is essentially contrast-free. Simulations show that quantitative images with minimal blurring are possible for petroleum reservoir core plug analysis when the dominant T_2 populations are longer than 5 ms. In samples where short T_2 relaxation time components are important, spin density imaging may be achieved with a centric scan SPRITE experiment or with the T_2 mapping SE-SPI method.

T_2 mapping SE-SPI technique permits fast determination of spatially resolved T_2 distributions in porous media with echo times of 500 μs or less. This technique permits generation of several thousand T_2 weighted images in several minutes. Given the short echo time and low field strength, the transverse life time distribution measured will be a true reflection of the fluid occupied pore size distribution. Determination of local T_2 distribution yields a simultaneous local measurement of the fluid content.

A practical application of these two methods, imaging a centrifuged core plug, has demonstrated that these two techniques provide reliable, robust and fast determination of the local saturation and spatially resolved T_2 distribution and together provide a promising new core analysis method.

The logarithm mean T_2, calculated from the T_2 distribution of individual pixels in the core plug, varies linearly with the water saturation. An empirical equation for the prediction of the irreducible water saturation in centrifuged core samples has been derived from permeability models.

The SE-SPI imaging techniques demonstrated provide quantitative analysis of local fluid saturation and the local T_2 distribution in porous media and are therefore very promising tools for petroleum reservoir core analysis and other areas of application.

5. Experimental

All MRI measurements were performed on a MARAN DRX spectrometer (Oxford Instruments Ltd., Oxford, UK) console with a wide bore, horizontal bore superconducting magnet (GE NMR 2T/31 magnet system, charged to 0.35 T). The home-made 3 axis micro-imaging gradient set was 3″ ID, with 0.67 Gauss/cm/A. A set of three Techron 8606 gradient amplifiers (GE medical system, Fremont, CA, USA) were employed for the imaging measurement. A home-made 45 mm inner diameter bird cage RF probe was used with a 300 W RF power amplifier (Resonance Instruments Ltd, Oxford, UK). All measurements were carried out at ambient magnet temperature 15 °C.

The Acciss, Unifit and Impstar processing packages developed in the IDL programming environment by the UNB MRI Centre were employed for image reconstruction, fitting and display. 2D Laplace Inversion Software (Magritek Ltd. New Zealand) was employed for determining the relaxation time distributions.

A Hermle bench top centrifuge, (Z513 K, Wehingen, Germany.) was employed for the centrifugation experiment. The centrifugation, for the T_2 distribution measurement, sample, was 2 h at 500 rpm. The SWIRR centrifugation experiment was undertaken in the same centrifuge for 48 h at 1000 rpm.

Reservoir core plug sandstone # 1 had a porosity of 20%, 5.5 cm length, 2.5 cm diameter. After water saturation, the relaxation times were $T_2^* = 778$ μs, $T_{2(1)} = 39.4$ ms, 53%; $T_{2(2)} = 228$ ms, 47%, with T_2 fit to a bi-exponential relaxation model. The T_1 was essentially single exponential at 100 ms.

The second reservoir core plug, sandstone sample # 2, had a porosity of 20%, 5.5 cm length, 2.5 cm diameter. After water saturation, the relaxation times were $T_2^* = 270$ μs, $T_{2(1)} = 4.2$ ms, 62%; $T_{2(2)} = 42$ ms, 38%, with T_2 fit to a bi-exponential relaxation model. The T_1 was essentially single exponential at 100 ms.

Hybrid SE-SPI imaging parameters were: 90° pulse length 17.5 μs; filter width 125,000 Hz; filter dead time 26 μs; FOV was 10 cm; maximum gradient strength was 5 G/cm. 64 *k*-space points were acquired with a phase encoding time of 150 μs; Single point acquisition was employed on the echo for image acquisition. Four signal averages were acquired in an imaging time of 20 s.

SE-SPI T_2 imaging parameters were: 90° pulse length 17.5 μs; phase encoding time was 150 μs; filter width was 125,000 Hz; filter dead time was 26 μs; The filter width was maintained at the values of the hybrid SE-SPI acquisition for experimental consistency. The FOV was 10 cm with a maximum gradient strength of 5 G/cm. Single point acquisition was employed on the echo with four signal averages. 1024 echoes (images) were acquired for sandstone # 1, 256 for sandstone # 2. The echo time was 500 μs, with an imaging time of 10 mins for sandstone # 1 and 5 min for sandstone # 2.

The SE-SPI phase cycle, for both imaging techniques, was a simple bulk CPMG phase cycle. The 90° pulse was $x, y, -x, -y$ with the 180° pulse set to $y, y, -y, -y$ for a receiver phase of $x, y, -x, -y$.

Acknowledgments

The authors thank R.P. MacGregor for his technical assistance. B.J.B. thanks NSERC of Canada, the Atlantic Innovation Fund, Petroleum Research Atlantic Canada, CFI and the Canada Chairs program for funding.

References

[1] S. Chen, K. Kim, F. Qin, A.T. Watson, Quantitative NMR imaging of multiphase flow in porous media, Magn. Reson. Imag. 10 (1992) 815–826.
[2] F. Marica, Q. Chen, A. Hamilton, C. Hall, T. Al, B.J. Balcom, Spatially resolved measurement of rock core porosity, J. Magn. Reson. 178 (2006) 136–141.
[3] B.J. Balcom, R.P. MacGregor, S.D. Beyea, D.P. Green, R.L. Armstrong, T.W. Bremmer, Single-point ramped imaging with T_1 enhancement (SPRITE), J. Magn. Reson. A 123 (1996) 131–135.
[4] Z. Zhang, A.E. Marble, B. MacMillan, K. Promislow, J. Martin, H. Wang, B.J. Balcom, Spatial and temporal mapping of water content across Nafion membranes under wetting and drying conditions, J. Magn. Reson. 194 (2008) 245–253.
[5] S. Gravina, D.G. Cory, Sensitivity and resolution of constant-time imaging, J. Magn. Reson. B 104 (1994) 53–61.
[6] Y. Cheng, M.B. MacMillan, R.P. MacGregor, B.J. Balcom, Direct detection of hydrocarbon displacement in a model porous soil with magnetic resonance imaging, Anal. Chem. 77 (2005) 1824–1830.
[7] Y. Cheng, ^{13}C Magnetic Resonance Imaging of Physico-Chemical Processes, UNB Ph.D. thesis, 2005 pp. 93–114.
[8] A.V. Ouriadov, R.P. MacGregor, B.J. Balcom, Thin film MRI—high resolution depth imaging with a local surface coil and spin echo SPI, J. Magn. Reson. 169 (2004) 174–186.
[9] S.D. Beyea, B.J. Balcom, I.V. Mastikhin, T.W. Bremner, R.L. Armstrong, P.E. Grattan-Bellew, Imaging of heterogeneous materials with a turbo spin echo single-point imaging technique, J. Magn. Reson. 144 (2000) 255–265.
[10] R.L. Kleinberg, W.E. Kenyon, P.P. Mitra, Mechanism of NMR relaxation of fluids in rock, J. Magn. Reson. 108 (1994) 206–214.
[11] Y. Song, S. Ryu, P.N. Sen, Determining multiple length scales in rocks, Nature 406 (2000) 178–181.
[12] R.L. Kleinberg, Utility of NMR T_2 distribution, connection with capillary pressure, clay effect, and determination of the surface relaxivity parameter ρ_2, Magn. Reson. Imag. 14 (1996) 761–767.
[13] D. Chang, H. Vinegar, C. Morriss, C. Straley, Effective porosity, producible fluid and permeability in carbonates from NMR logging, The Log Analyst 38 (1997) 60–72.
[14] G.R. Coates, D. Marschall, D. Mardon, J. Galford, A new characterization of bulk-volume irreducible water using magnetic resonance, The Log Analyst 39 (1998) 51–63.

[15] C.S. Poon, R.M. Henkelman, Practical T_2 quantization for clinical applications, J. Magn. Reason. Imag. 2 (1992) 541–553.
[16] A.P. Crawley, M.L. Wood, R.M. Henkelman, Elimination of transverse coherences in FLASH MRI, Magn. Reson. Med. 8 (1988) 248–260.
[17] A.A. Maudsley, Modified Carr-Purcell-Meiboom-Gill sequence for NMR imaging Fourier imaging applications, J. Magn. Reson. 69 (1986) 488–491.
[18] X. Wan, D.L. Parker, J.N. Lee, H.R. Buswell, G.T. Gullberg, Reduction of phase error ghosting artifacts in thin slice fast spin echo imaging, Magn. Reson. Med. 34 (1995) 632–638.
[19] T. Gullion, The effect of amplitude imbalance on compensated Carr–Purcell sequence, J. Magn. Reson. 101 (1993) 320–323.
[20] H.T. Edzes, D. Dusschoten, H.V. As, Quantitative T_2 imaging of plant tissues by means of multi-echo MRI microscopy, Magn. Reson. Imag. 16 (2) (1998) 185–196.
[21] L.L. Latour, R.L. Kleinberg, P.P. Mitra, C.H. Sotak, Pore-size distributions and tortuosity in heterogeneous porous media, J. Magn. Reson. 112 (1995) 83–91.
[22] R.L. Kleinberg, M.A. Horsfield, Transverse relaxation processes in porous sedimentary rock, J. Magn. Reson. 88 (1) (1990) 9–19.
[23] P. Wong, Methods in the Physics of Porous Media, Academic Press, New York, 1999.
[24] D.J. Goodyear, M. Shea, S.D. Beyea, N.J. Shah, B.J. Balcom, Single point measurements of magnetic field gradient waveform, J. Magn. Reson. 163 (2003) 1–7.
[25] K. Deka, M.B. MacMillan, A.V. Ouriadov, I.V. Mastikhin, J.J. Young, P.M. Glover, G.R. Ziegler, B.J. Balcom, Quantitative density profiling with pure phase encoding and a dedicated 1D gradient, J. Magn. Reson. 178 (2006) 25–32.
[26] M.C. Jeruchim, P. Balaban, K. Sam Shanmugan, Simulation of Communication Systems, Plenum Press, New York, NY, USA, 1992.
[27] Q. Chen, B.J. Balcom, Measurement of rock core capillary pressure curves using a single-speed centrifuge and one dimensional magnetic resonance imaging, J. Chem. Phys. 122 (2005) 214720–214728.
[28] L.W. Lake, E.D. Holstein, Petroleum Engineering Handbook, Society of Petroleum Engineers, TX, USA, 2007, pp. V 289–V 356.